Encoding Light Intensity by the Cone Photoreceptor Synapse

Report

Sue-Yeon Choi,[1] Bart Borghuis,[2] Ruth Rea,[1]
Edwin S. Levitan,[3] Peter Sterling,[2]
and Richard H. Kramer[1],*
[1]Department of Molecular and Cell Biology and
    the Helen Wills Neuroscience Institute
University of California, Berkeley
Berkeley, California 94720
[2]Department of Neuroscience
University of Pennsylvania
Philadelphia, Pennsylvania 19104
[3]Department of Pharmacology
University of Pittsburgh
Pittsburgh, Pennsylvania 15261

Summary

How cone synapses encode light intensity determines the precision of information transmission at the first synapse on the visual pathway. Although it is known that cone photoreceptors hyperpolarize to light over 4–5 log units of intensity, the relationship between light intensity and transmitter release at the cone synapse has not been determined. Here, we use two-photon microscopy to visualize release of the synaptic vesicle dye FM1-43 from cone terminals in the intact lizard retina, in response to different stimulus light intensities. We then employ electron microscopy to translate these measurements into vesicle release rates. We find that from darkness to bright light, release decreases from 49 to ∼2 vesicles per 200 ms; therefore, cones compress their 10,000-fold operating range for phototransduction into a 25-fold range for synaptic vesicle release. Tonic release encodes ten distinguishable intensity levels, skewed to most finely represent bright light, assuming release obeys Poisson statistics.

Introduction

The outer segment of cone photoreceptors generates a finely graded hyperpolarization whose magnitude increases over 4–5 log units of light intensity. This information is transmitted by the synaptic terminal of cones, which tonically releases transmitter in the dark and suppresses release in the light. Because neurotransmitter is packaged in synaptic vesicles that are released in a quantal manner, the dynamic range of vesicle release rates governs how precisely changes in intensity can be signaled to postsynaptic neurons. Moreover, the shape of the intensity-release relationship determines how equally intensity is represented across the operating range of the cone. Despite its central importance for understanding visual information transfer, the input-output relationship of cones has not been measured directly.

Electrophysiology has been the main approach for understanding the steps linking photon capture to synaptic transmission. Light-induced electrical responses in outer segments (Normann and Werblin, 1974; Attwell et al., 1982; Schnapf et al., 1990) and regulation of voltage-gated Ca^{2+} channels in cone terminals (Barnes and Hille, 1989; Verweij et al., 1996; Savchenko et al., 1997; DeVries, 2001) have been investigated. Membrane capacitance measurements have revealed the Ca^{2+} dependence of synaptic vesicle release (Rieke and Schwartz, 1994; Kreft et al., 2003; Thoreson et al., 2004). However, these techniques have not been utilized to study how light regulates tonic vesicle release.

Instead, an indirect assay has been used to investigate the relationship between light and synaptic vesicle release in cones. Electrical recordings from postsynaptic bipolar cells reveal voltage fluctuations that are reduced by light (Ashmore and Copenhagen, 1983). These fluctuations are too large to be caused by variations in the activation of individual glutamate receptors and thus may be the consequence of vesicle fusion in cones (Berntson and Taylor, 2003). However, bipolar cell noise is measured several steps removed from synaptic vesicle release and may be influenced by other processes. For example, the light-induced hyperpolarization in cones not only suppresses vesicle release but also reduces the activity of glutamate transporters in the terminal (Gaal et al., 1998). Features of the circuitry of the outer retina, including electrical coupling between photoreceptors, convergence of many photoreceptors onto individual bipolar cells, and feedback from horizontal cells onto cones (Wu, 1994) can further complicate the interpretation of bipolar cell noise. Thus, some type of direct measurement from the cone terminal is needed to quantify unambiguously the relationship between light and synaptic vesicle release.

Here, we use direct optical measurements to determine the input-output relation of cones. We showed previously that the fluorescent dye FM1-43 labels selectively synaptic vesicles in cone terminals and that unloading of the dye reflects Ca^{2+}-dependent exocytosis (Rea et al., 2004). To explore how light controls release, we now use 2-photon microscopy, which is advantageous because (1) it uses invisible (infrared) light to excite the dye, allowing release to be monitored without triggering phototransduction; and (2) it can focus deeply into the intact retina. By repeatedly scanning with infrared light, we examine how different intensities of visible light regulate dye release. Then, we convert dye release into vesicle release by electron microscopy to count the releasable synaptic vesicles in a terminal. We find that the synapse compresses the 4- to 5-log unit range of phototransduction into release rates of 0 to 250 vesicles per second, limiting the contrast sensitivity of downstream neurons in the visual pathway.

Results

Visualizing Synaptic Vesicles in Cones with FM1-43

To visualize synaptic vesicles in cones, we loaded the all-cone retina of the anole lizard with FM1-43. Dye was loaded in the dark, when exocytosis from cones is
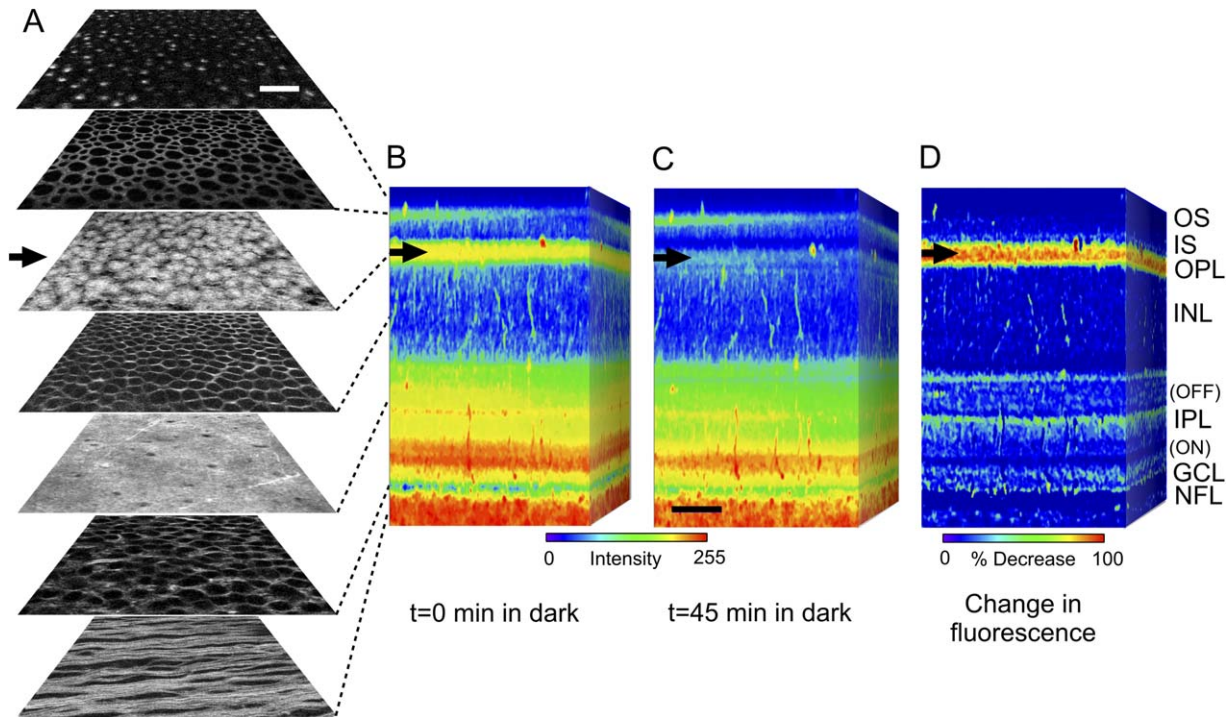
*Correspondence: rhkramer@berkeley.edu

Figure 1. FM1-43 in the Intact Retina

(A) Fluorescence images of a flat-mounted retina loaded with FM1-43. Seven different planes of focus (Z sections) are shown, extending from cone outer segments in the outer retina (top) to the nerve fiber layer (bottom) of retinal ganglion cells in the inner retina. Dashed lines show approximate corresponding depths in (B) and (C). The OPL is indicated with an arrow. Scale bar, 10 μm.

(B and C) Virtual cross-sections of the retina generated from 700 Z sections scanned 300 nm apart through the retina. Fluorescence intensity is color coded as shown below. Scale bar, 30 μm. (B) Retina shortly after loading. (C) The same retina 45 min after unloading in the dark. Note the dramatic loss of dye in the OPL (arrows) and the modest loss in the OFF-sublamina of the IPL.

(D) Difference image (C−B)/(B) showing fractional loss of fluorescence after unloading in the dark, color coded as shown below. OS, cone outer segment; IS, cone inner segment; OPL, outer plexiform layer; INL, inner nuclear layer; IPL, inner plexiform layer; GCL, ganglion cell layer; NFL, nerve fiber layer.

continuous. Vesicles retrieved from the plasma membrane by compensatory endocytosis incorporate the dye, resulting in bright labeling in cone terminals (Rea et al., 2004). To excite FM1-43 fluorescence without exposing the tissue to visible light, we used a train of 860 nm pulses of infrared light from a two-photon microscope.

Scanning through the layers of the retina, we could identify the array of cone terminals in the outer plexiform layer (OPL, arrows in Figures 1A–1D), which had accumulated dye. The inner plexiform layer (IPL), which contains synaptic vesicles in presynaptic terminals of bipolar and amacrine cells, also showed bright labeling. In contrast, the nonsynaptic inner and outer nuclear layers showed much less labeling. Ganglion cell bodies also excluded the dye, but their axons in the nerve fiber layer (NFL) showed intense labeling, perhaps reflecting passive diffusion into their cut ends.

Reconstructions of a stack of 700 serial optical sections produced a virtual cross-section of the retina, showing layers that had accumulated FM1-43 (Figure 1B). Retinas held in darkness for 45 min after FM1-43 loading retained dye in most layers, except for the OPL (Figure 1C). (See Movies S1 and S2 for rotating 3D reconstructions of this retina.) We subtracted the image stack in Figure 1C from that in Figure 1B. The resulting difference image shows that darkness promotes nearly complete loss of dye from cone terminals in the OPL

(Figure 1D). Dye was also released from the OFF sublamina of the IPL, which includes presynaptic terminals of OFF bipolar cells that are tonically depolarized and releasing transmitter in the dark. The ON sublamina, which includes ON bipolar cell terminals that are hyperpolarized in the dark, showed little loss of dye.

Measuring Light-Regulated Release of FM1-43
To measure the rate of dye loss from cone terminals, we focused on the OPL and scanned repeatedly over 20 min in the dark. We found that all of the terminals progressively released their dye over this time (Figure 2A). About 10% of the dye was released over the first minute, 80% over 20 min, and the loss could be fit with a single exponential function with a time constant of ∼10 min (Figure 2B). Exposure to bright visible light strongly suppressed dye release, with only 5% loss over 20 min and a time constant of 266 min.

The cone's electrical response to light spans 4- to 5-log units of intensity (Normann and Werblin, 1974; Attwell et al., 1982; Schnapf et al., 1990). By following dye loss during steady illumination over this range, we found that as intensity decreased, release was accelerated in a graded manner. At each light level, the release rate could be fit accurately with a single exponential function. This is consistent with both exocytosis and endocytosis occurring at a constant rate, which would progressively
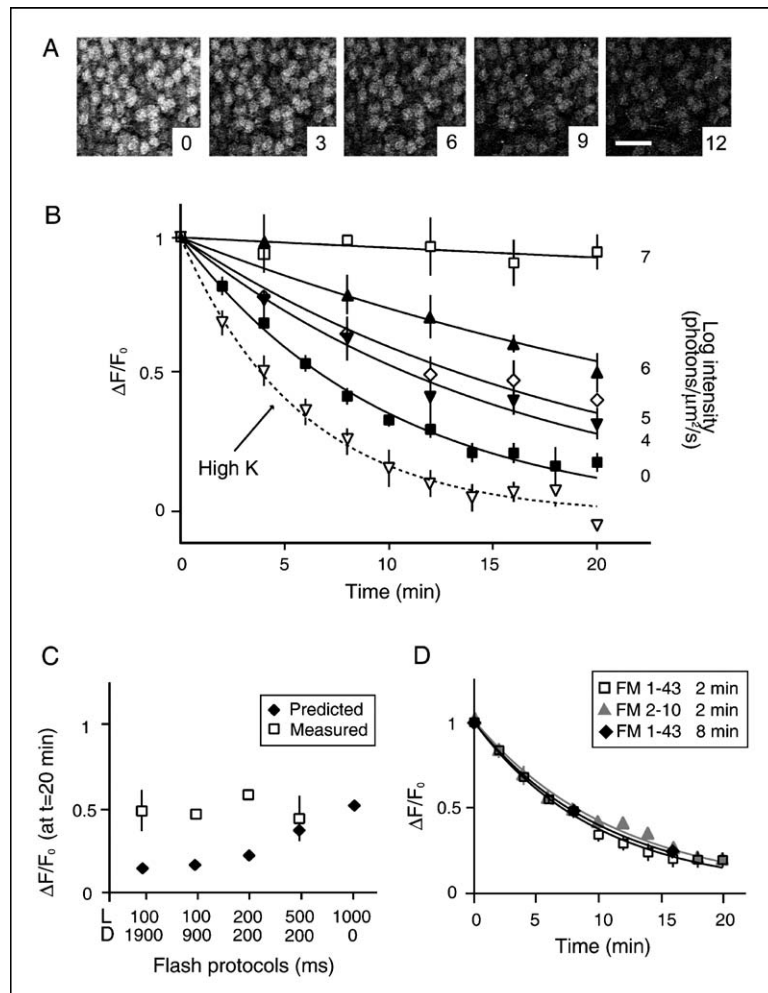
Figure 2. Regulation of Exocytosis by Light and Dark

(A) Fluorescence images showing unloading of FM1-43 in the dark from cone terminals in a Z section through the OPL. Two-photon scans were applied at 3 min intervals. The numbers show elapsed time in minutes. Scale bar, 20 μm.

(B) Unloading of FM1-43 in the dark, in steady light of different intensities (indicated on the right), or after application of high K$^+$. Continuous curves show single exponential fits to the data with release time constants (in min) of 10.3 (dark), 17.5 (log 4), 22.0 (log 5), 35.5 (log 6), 266.3 (log 7), and 5.9 (high K$^+$). n = 5–9 for each condition.

(C) Effects of temporal resolution on release. Measured (open squares) and predicted (filled diamonds) percent of dye released after exposure to repeated flashes for 20 min. The length of light (L) and dark (D) periods are indicated on the abscissa. Light intensity of 10^6 photons/μm^2/s was used. n = 2–6.

(D) Dye release accurately reflects exocytosis in the dark. FM1-43 (open squares) and FM2-10 (gray triangles) release rates are similar, suggesting no significant contribution from kiss-and-run exocytosis. Release of FM1-43 in the dark is similar with 2 min (open squares) or 8 min (filled squares) 2-photon scans, indicating that infrared exposure did not alter release. Continuous lines show single exponential fits to the data. n = 4–5. Variability among data is expressed as mean ± SEM.

decrease the proportion of labeled vesicles in the terminal. This result suggests that in each experiment, light adaptation had already reached steady state at the time when the release measurement was initiated (2 min after the onset of steady illumination). Decreasing our brightest light intensity (10^7 photons/μm^2/s) by 1,000-fold accelerated release by ~15 fold, indicating that different steady intensities are represented by different tonic release rates with rather low precision. This signal compression at the cone terminal should not be confused with the effects of light adaptation in the outer segment, which expands the cone's light sensitivity to match the level of background illumination. The modest changes in release rate with steady background light preserves much of the operating range of release, which could be exploited for transmitting information about stimuli with higher temporal contrast.

Consistent with this, the cone terminal can release at rates that exceed our measured steady dark rate. When cone terminals were depolarized beyond their dark potential by applying high (50 mM) K$^+$, dye loss was further accelerated by 1.6-fold (Figure 2B), presumably to near the maximal steady release rate. These higher release rates might occur transiently when a cone senses rapid changes in intensity, for example, when the eye flicks about a scene.

To further evaluate the effects of temporal contrast, we measured dye loss while stimulating the retina with repeated flashes of light (Figure 2C). If temporal contrast had no effect, the total amount of dye released over a given time should equal the sum of dye released during all intervals of light and darkness, which can be predicted from the measured steady rates. When 500 ms flashes were used to temporarily suppress release with bright flashes (10^6 photons/μm^2/s) (Figure 2C) or dimmer flashes (10^5 photons/μm^2/s; data not shown), measured release did match predicted release. However, with shorter flashes (100–200 ms), suppression of release was ~2-fold greater than predicted (~85% versus ~50% over 20 min). The additional suppression of release caused by brief flashes is consistent with the known time course of light adaptation in the outer retina, ~100 ms (Hayhoe et al., 1992). Presumably, a brief flash decreases the average release rate more than a longer flash because it causes less light adaptation, which would tend to restore the dark rate. Hence, temporal contrasts are synaptically encoded more finely than steady intensities.

Control experiments confirm that FM1-43 loss accurately reports synaptic vesicle exocytosis. If release events were of the "kiss-and-run" variety, in which the vesicle membrane briefly and incompletely fuses with the plasma membrane, they would unload incompletely
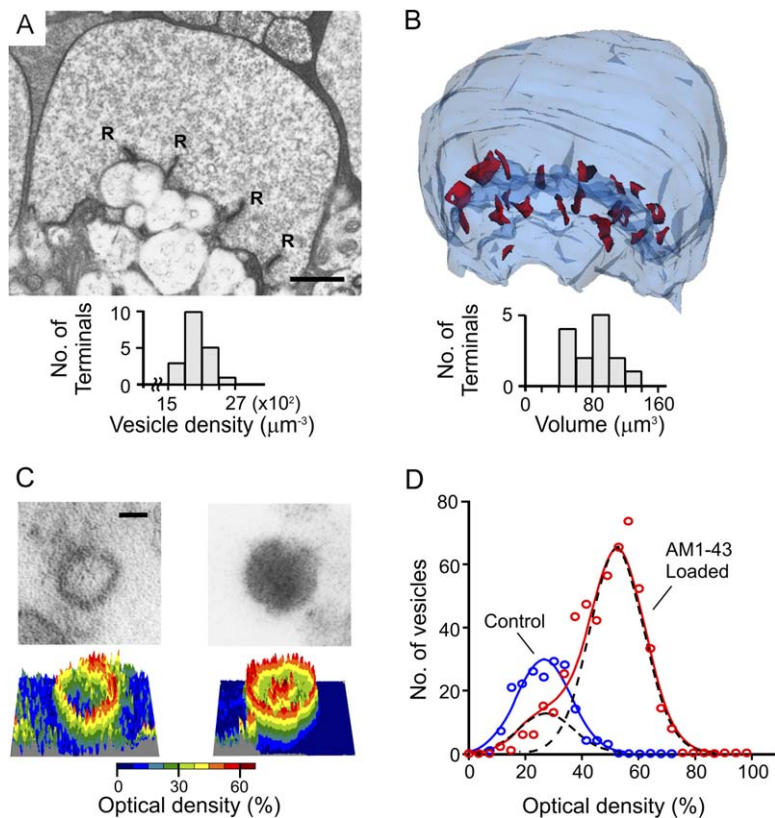
Figure 3. Determination of the Size of Cycling Pool of Vesicles in the Cone Synapse

(A) Density of vesicles was calculated from ultrathin EM sections, 0.08 μm thick. R, synaptic ribbon. Scale bar, 1 μm. Inset shows the distribution of densities in 19 sections.

(B) 3D reconstruction of a cone terminal from a series of ultrathin EM sections. Ribbons are in red. Inset shows the distribution of volumes from 14 terminals.

(C) Electron micrographs showing that control vesicles (left) have a dark perimeter and a bright center; AM1-43 photoconverted vesicles (right) have a dark perimeter and an even darker center. Color-coded optical density profiles for each are shown below. Scale bar, 20 nm.

(D) Amplitude histogram of optical density values of vesicles from control (blue circles) and AM1-43 photoconverted terminals (red circles) are fitted with a single Gaussian (blue line) or the sum of two Gaussians (dashed and red lines), respectively.

because FM1-43 dissociates slowly from membranes (Stevens and Williams, 2000). However, FM2-10, a more hydrophilic analog, is fully released during kiss-and-run exocytosis (Klingauf et al., 1998). We found that the release rates of FM1-43 and FM2-10 from cone terminals in the dark are indistinguishable (Figure 2D). Consequently, cone vesicle release allows complete FM1-43 unloading and, therefore, full vesicle fusion.

We also considered whether the infrared pulses used to measure FM1-43 might have triggered phototransduction and, thus, spuriously affected release. To control for this, we took 2-photon scans of the cone terminals at either 2 min or 8 min intervals (Figure 2D). Unloading rates were the same with both protocols, even though there was a 4-fold difference in total exposure to infrared light. We also compared the rate of FM1-43 loading in complete darkness with the rate of unloading, measured by repeated scans with the infrared laser. At steady state, the rates of endocytosis and exocytosis should be the same, so the rates of dye loading and unloading should be equal. Dye accumulation in the dark, which was abruptly terminated by applying Ca^{2+}-free saline to the retina, had a time constant of 8.1 ± 2.5 min (n = 5), similar to the unloading time constant of 9.9 ± 0.2 min (n = 9). Taken together, these results strongly suggest that the 2-photon scan had no significant effect on the FM1-43 release rate.

Converting Dye Release into Vesicle Release

To calculate the rate of vesicle release from the rate of dye release, we needed to know the number of synaptic vesicles that initially contained the dye. The number of labeled synaptic vesicles can be determined with elec-

tron microscopy. To quantify the total number of vesicles per terminal (V_T), we measured the density of vesicles per unit volume from ultrathin sections (2,007 $\pm$ 262 vesicles per μm^3, n = 19) (Figure 3A), and we measured the total terminal volume from complete 3D reconstructions of cone terminals (84 ± 23 μm^3, n = 14) (Figure 3B). From these measurements, we determined that V_T is ~170,000.

Conventional synapses possess a large reserve pool of synaptic vesicles (75%–85% of the total) (Pyle et al., 2000; Richards et al., 2003) that are not easily released by stimulation and do not usually participate in the vesicle cycle. To determine what proportion of vesicles participates in the cone's vesicle cycle, we again used electron microscopy. Cone terminals were first loaded with AM1-43, a glutaraldehyde-fixable analog of FM1-43 (Renger et al., 2001). Retinas were incubated with the dye for >15 min, sufficient to saturate loading. After fixation, AM1-43 could be localized subcellularly by subsequently adding diaminobenzidine and illuminating intensely with a laser to generate an electron-opaque reaction product (Henkel et al., 1996). Synaptic vesicles from control terminals showed electron-lucent centers (Figure 3C), whereas the centers of vesicles from a "photoconverted" terminal were often more electron dense, as shown previously at nonribbon synapses (Harata et al., 2001). The distribution of optical density values of vesicles from control terminals could be fit with a single Gaussian function, but those from photoconverted terminals required a double Gaussian (Figure 3D). The smaller peak (14%) represents electron-lucent vesicles, like those in control terminals, whereas the larger peak (86%) represents electron-dense vesicles. Therefore,
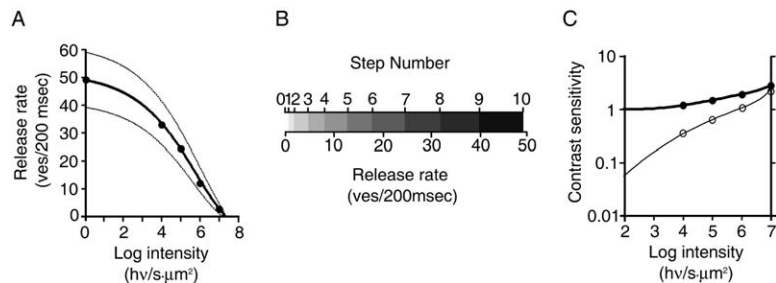
Figure 4. Intensity Coding at the Cone Synapse

(A) The input-output relation of the cone synapse. Vesicle release rates (filled circles) at different light intensities are fitted with a sigmoidal function (thick line). Thin lines represent confidence levels from a single-trial two-alternative forced-choice test.

(B) Cone vesicle release can encode a limited number (10) of distinct gray scales of light intensity. Steps show increments of intensity that can be reliably distinguished by changes in release rate, assuming Poisson statistics apply.

(C) Predicted contrast sensitivity of the cone photoreceptor, by using an ideal observer model, with increments of light above background (thin line) and decrements below background (thick line).

the cycling fraction of vesicles is 86%, similar to the percentage of vesicles in cone terminals that are freely mobile, as determined by fluorescence recovery after photobleaching (Rea et al., 2004).

Encoding Light Intensity by Synaptic Vesicle Release

We calculated the vesicle release rate at different light intensities by applying the following equation:

$$R_I = (dF/F) \, V_T \cdot C$$

in which R_I is the release rate at a given intensity, dF/F is the initial rate of dye loss for that intensity (10% per minute in darkness) (see Figure 2B), V_T is the total number of vesicles per terminal (170,000), and C is the fraction that are available for release (86%). Calculating vesicle release rates, we find that in complete darkness, R was 246 vesicles s^{-1}, or 49 vesicles over 200 ms (Figure 4A). Electron microscopic reconstructions (see Figure 3B) show that cone terminals contain about 25 ribbon-type active zones (24, 24, and 26 in three different terminals). Therefore, in darkness, each ribbon tonically releases about 10 vesicles s^{-1}. The maximal rate from a cone terminal in high K$^+$ was 389 vesicles s^{-1}, or about 16 vesicles s^{-1} from each ribbon. R was relatively insensitive to modulation by dim light (<10^4 photons/μm^2/s) but decreased progressively with intensities >10^4 photons/μm^2/s and approached zero at about 10^7 photons/μm^2/s.

If vesicle release from cones were a stochastic process that obeyed Poisson statistics, the standard deviation of the vesicle release rate would equal the square root of the release rate. Under these conditions, both the average release rate and its variability would decrease with illumination. Figure 4B shows how these features constrain the encoding of light intensity. To distinguish one light level from another, the difference in release rates must reliably exceed the variability in these rates. Starting in darkness, release statistics would allow distinction of ten steps of intensity over a 200 ms interval (the integration time of bipolar cells) (Ashmore and Copenhagen, 1983). However, the assignment of these steps is skewed to more accurately represent brighter light.

This intensity code generated in the photoreceptor dictates the contrast sensitivity of a downstream bipolar

cell or how sensitively it can detect a change in intensity. To quantify the contrast sensitivity, we used an ideal observer model (Banks et al., 1987; Geisler, 1989) based on the measured decline in release rate and the predicted decline in release variability as intensity increases. Overall, temporal contrast sensitivity was better for light decrements than for light increments (Figure 4C), matching psychophysical observations (Bowen et al., 1998; DeMarco et al., 1994). As background illumination increased, temporal contrast sensitivity improved for increments, but changed relatively little for decrements, also consistent with psychophysical observations in humans (Patel and Jones, 1968).

Discussion

Directly Measuring How Light Affects Tonic Exocytosis from the Cone Synapse

Here, we have directly measured how tonic vesicle release from cones is regulated by light intensity. We measure a release rate in darkness of 246 vesicles s^{-1}. This is within a factor of three of the higher release rates estimated from postsynaptic noise analysis (Ashmore and Copenhagen, 1983; Berntson and Taylor, 2003), which could have resulted from an underestimate of cone convergence onto bipolar cells. We find that steady light reduces the vesicle release rate, with the input-output relation being skewed to more accurately reflect the brighter end of the cone's operating range. Saturating light completely suppresses release. However, even with exposure to relatively dim light (e.g., 10^4 photons/μm^2/s) for tens of minutes, the tonic release rate was reduced significantly, indicating that steady-state light adaptation is incomplete. Cones respond and transmit best when changes in illumination are rapid, but our results show that persistent changes in intensity can indeed be communicated by the cone synapse.

In evaluating our measurements, we considered possible sources of error. First, if vesicles fused incompletely (kiss-and-run), their FM1-43 dye would be released only partially, causing underestimation of the release rate. However, FM2-10, an analog that dissociates more rapidly, gave the same result as FM1-43 (Figure 2D), confirming that release is by full fusion. Second, spurious excitation of the cone photopigment by 2-photon laser would also cause underestimation of release rates.

However, quadrupling laser exposure time did not alter the release rate. Moreover, rates of FM1-43 loading in darkness and unloading measured with repeated laser scanning were similar. These observations demonstrate that 2-photon scanning did not perturb release.

Euler et al. (2002) found that 2-photon imaging of a Ca^{2+} indicator dye did trigger electrical responses in rabbit amacrine neurons, indicating some excitation of photoreceptors. But, their experiments required continuous laser scanning to discern relatively rapid changes in intracellular Ca^{2+}. In contrast, we could use infrequent scans (e.g., every 2 min) because FM1-43 release occurs over many minutes. Also, because the fluorescence of FM1-43-loaded cone terminals was bright, we could use low intensity, high-speed scans, with a very brief dwell time per cone ($\sim$0.5 ms). Finally, the amacrine cell responses probably resulted from excitation of rods, which are much more sensitive to light than cones. Whereas rabbit photoreceptors are mostly rods (>90%), the anole lizard photoreceptors are only cones, reducing the chance of spurious activation.

FM1-43 reports release only with low temporal resolution because even in darkness, dye unloading requires several minutes. Therefore, our calculated range of release rates applies to constant levels of illumination, when light adaptation has reached steady state. We examined how temporal contrast affects the average release rate (see Figure 2C), but we could not resolve how release is rapidly modulated during or after a light flash. In fact, the transient effects of light and dark probably exceed what we measure in steady-state light and dark conditions. Consistent with this, cones generate a depolarizing afterpotential after a light flash and can even generate spikes (Schnapf et al., 1990). Moreover, the resulting rise in intracellular Ca^{2+} concentration may be further amplified by Ca^{2+}-induced Ca^{2+} release (Krizaj et al., 2003).

Capacitance measurements show that the cone terminal is capable of release rates much higher than those shown here. A large depolarization (to −10 mV) can elicit a transient burst of release that exceeds 5,000 vesicles in 10 ms (Rabl et al., 2005). This probably reflects fusion of primed vesicles that are already docked to their release sites, which must be orders of magnitude more likely to fuse than other vesicles. In contrast, vesicle release rates measured with FM1-43 reflect many more steps in the vesicle cycle, including vesicles diffusing to and interacting with the synaptic ribbon, in addition to the final events of membrane fusion. Thus, capacitance measurements and FM1-43 provide different, but complementary, insights into how vesicle release is regulated.

Although our approach has limited temporal resolution, it does offer high spatial resolution. Optical measurements allow visualization of release from individual terminals. Simultaneously, it allows measurements of activity across a wide array of terminals in the intact retina. Revealing synaptic activity in an entire slab of neural tissue could be beneficial for understanding circuit interactions in the retina, for example, lateral inhibition by the horizontal cell feedback synapse on cone terminals.

Role of the Synaptic Ribbon
If synaptic ribbons were a required gateway for tonic release, then the release rate would depend on (1) the encounter rate between vesicles and ribbons and (2) the rate at which vesicles are processed by ribbons for fusion with the plasma membrane. We estimated the encounter rate from a three-dimensional diffusion model with a vesicle diffusion coefficient of 1.1×10^{-9} cm^2/sec (Rea et al., 2004), a density of synaptic vesicles of $\sim$2,000/μm^3 (Figure 3A), 85% of the vesicles being releasable (Figure 3D and Rea et al., 2004), and a total ribbon surface area of 6 μm^2 (Figure 3B). We estimate that $\sim$3,800 vesicles s^{-1} encounter the synaptic ribbons, about 15 times faster than the release rate in the dark. Hence, the rate at which vesicles encounter the ribbon does not limit the release rate. It follows that other events, such as priming, which may occur on the ribbon, or fusion, which occurs at the plasma membrane, must be rate limiting for release. Elevated internal Ca^{2+}, which is the ultimate trigger for release, does not affect vesicle mobility (Rea et al., 2004), so it should not affect the ribbon encounter rate. Hence the linear relationship between Ca^{2+} concentration and release in photoreceptors (Thoreson et al., 2004) is consistent with a single Ca^{2+}-sensitive step, which must occur after vesicles encounter the ribbon.

Encoding of Light Intensity by Vesicle Release
Compared to the outer segments, which encode a >10^4 range of light intensities into an electrical response, the cone terminal has a low "bit depth" because its representation of light by vesicle release rate is rather coarse. The full operating range for the cone is only 246 vesicles s^{-1}, several orders of magnitude lower than the outer segment's photoisomerization rate in bright light (>10^6 s^{-1}) (Rodieck, 1998). The threshold intensity for regulating synaptic vesicle release is near 10^2 photons/μm^2/s, similar to the electrophysiologically-measured threshold for generating a voltage response in cones (Normann and Werblin, 1974; Attwell et al., 1982; Schnapf et al., 1990). Above 10^4 photons/μm^2/s, the slope of the relationship between log intensity and release rate is constant, such that each log unit of intensity is represented by an equal number of released vesicles. Thus, in bright light, synaptic transfer from cones obeys the Weber-Fechner law, consistent with a long history of psychophysical observations (Purves et al., 2004).

The relationship between intensity and release parallels a similar relationship between light intensity and cone photovoltage, except that the amplitude of hyperpolarization is sigmoidal and tends to level off gradually at high intensities (Normann and Werblin, 1974; Attwell et al., 1982; Schnapf et al., 1990). The truncated sigmoidal shape of the intensity versus release rate curve suggests that in very bright light, as the release rate approaches zero, the synapse "clips" the light response, as suggested previously for rods (Attwell et al., 1987). Consistent with this, the phototransduction operating range of light-adapted cones extends beyond 10^8 photons/μm^2/s (Normann and Werblin, 1974; Perlman and Normann, 1998), whereas we find that release is completely suppressed near 10^7 photons/μm^2/s.

Assuming that vesicle release is stochastic and obeys Poisson statistics, our model predicts that to full-field illumination, the cone synapse would have a maximal contrast sensitivity of $\sim$3. This resembles values from full-field illumination of primate parvocellular ganglion

cells (~4) (Derrington and Lennie, 1984), which in the fovea, receive input from a single cone (Calkins et al., 1994). To the same stimulus, a magnocellular ganglion cell with inputs from about 50 cones has a contrast sensitivity of ~8 (Derrington and Lennie, 1984), consistent with the expected improvement in signal-to-noise ratio by convergent inputs (Demb et al., 2004). To spatial patterns, the parvocellular ganglion cell exhibits greater contrast sensitivity, up to ~10, depending on the spatial frequency (Derrington and Lennie, 1984). This is consistent with the cone expanding its dynamic range of vesicle release, presumably as a consequence of changes in lateral interactions by horizontal cells feedback synapses. These might elevate release above the dark rate by enhancing the voltage-gated Ca^{2+} current in cone terminals (Verweij et al., 1996).

On the other hand, vesicle release may not be purely stochastic. There is electrophysiological evidence for coordinated multivesicular release at ribbon synapses from photoreceptors (Maple et al., 1994) and bipolar cells (Singer et al., 2004), perhaps mediated by compound fusion events, in which vesicles fuse with one another before fusing with the plasma membrane (Parsons and Sterling, 2003). This might coordinate release within an active zone (i.e., at a ribbon) while leaving different active zones able to release independently. Feedback inhibition of cone neurotransmitter release by protons liberated from fusing synaptic vesicles (Barnes et al., 1993) might also decrease the randomness of release. In this scenario, each released vesicle would delay subsequent release events by transient extracellular acidification, briefly inhibiting voltage-gated Ca^{2+} channels and thus delaying Ca^{2+}-dependent exocytosis (DeVries, 2001; Vessey et al., 2005). These ideas need to be tested experimentally, which will probably require visualization of the release of individual vesicles and synaptic ribbons in living terminals (Zenisek et al., 2000, 2004).

Psychophysical experiments suggest that humans are more sensitive at detecting light decrements than increments (Bowen et al., 1998; DeMarco et al., 1994). Also, sensitivity to decrements is rather constant at different background intensities, whereas sensitivity to increments improves with intensity. These behavioral observations have not previously been explained, but our ideal observer model (Figure 4C) suggests these features of human visual sensitivity are set by the first synapse on the visual pathway.

Experimental Procedures

Retinal Preparation and Dye Loading
All procedures were approved by the UC Berkeley Animal Care and Use Committee. Eyes were obtained from the lizard *Anolis segrei* maintained on a 12:12 light:dark cycle. After 1 hr of dark adaptation, the eye was hemisected, and the retina was removed in the dark, with the retinal pigment epithelium (RPE) attached. For dye unloading experiments, the retina was mounted onto filter paper RPE-side down and bathed in lizard saline containing 30 μM FM1-43 from 45 min to 3 hr followed by a 5 min wash with 1 mM Advasep-7, as described previously (Rea et al., 2004). Fluorescence was normalized to 1.0 at the onset of experiments and to 0.0 at the end of experiments, after adding high K+ saline to release all releasable vesicles. For dye loading experiments, 30 μM FM1-43 was added to intact retina before mounting. Retinas were prepared at 21°C in complete darkness with the aid of an IR converter. High K^+ saline contained 50 mM KCl, iso-osmotically replacing NaCl.

Imaging
We used a Zeiss 510 confocal system equipped with a MaiTai (Spectra Physics, Mountain View, CA) mode-locked Ti:sapphire laser (860 nm) and a 40× achroplan, 0.8 NA water-immersion objective. Images were acquired with Zeiss LSM software and analyzed with Scion Image software. 700 optical sections focused 300 nm apart were obtained to image the entire retina. 3D reconstructions of the FM-loaded retina were made with Imaris software (Bitplane). We imaged a square region of the OPL (230 × 230 μm) for release experiments. White light from a halogen bulb with an intensity of 10^7 photons/μm²/s was used for illumination and attenuated with neutral density filters. An electronic shutter controlled flash duration and frequency.

Electron Microscopy
Lizard retinas were fixed and prepared for EM as described previously (Rea et al., 2004). Vesicle density in cone terminals was calculated from ultrathin EM sections. Average terminal volume was calculated from 3D reconstructions of the cone synaptic terminal, which were made with Reconstruct software (Synapse Web). AM1-43-loaded retinas were photoconverted (Rea et al., 2004). Images of EM sections from these retinas were digitized, and the fraction of vesicles that were labeled was determined based on optical density (average pixel value; n = 684). Unless noted otherwise, variability among data is expressed as mean ± SEM.

Calculations and Modeling
For each level of steady illumination, fluorescence decrease was fitted with a single exponential equation,

$$F_t = F_0 \cdot e^{(-t/\tau_i)} + F_\infty$$

In which F_t is fluorescence intensity at time t, F_0 is the initial fluorescence intensity, F_∞ is fluorescence at $t = \infty$, and τ_i is the release time constant at light intensity i. Normalizing the fluorescence measurements ($F_0 = 1$, $F_\infty = 0$) simplifies the equation to

$$F_t = e^{(-t/\tau_i)}$$

To predict release during the repeated light flash protocols, we set release rates within each light and dark interval to those measured during steady-state conditions. Then, the amount of dye remaining at time t, is

$$F_{t.flash} = \left(e^{(-x_d/\tau_d)} \cdot e^{(-x_l/\tau_l)} \right)^n,$$

in which x_d and x_l are the times spent in dark and light, respectively, during each flash cycle, τ_d and τ_l are the release time constants in steady dark and light, and n is the total number of flash duty cycles.

Assuming that synaptic transmission obeys Poisson statistics, the number of distinguishable light levels represented by the synapse follows from

$$R_{i+1} = R_i - (1.4 \cdot \sqrt{R_i})$$

in which R_i is the number of vesicles released at a given intensity, and R_{i+1} the number of vesicles released at the smallest reliably detected intensity change. Threshold was set at 1.4 standard deviations between probability density functions for the two stimuli, as in equivalent psychophysical experiments.

Contrast sensitivity was computed with an ideal observer model (Banks et al., 1987; Geisler, 1989) that detected intensity increments (positive contrast) or decrements (negative contrast) in a single-interval two-alternative forced choice paradigm. By numerical simulation, contrast sensitivity was computed from the ratio of the background intensity and the smallest intensity increment and decrement that could be detected reliably (68% correct).

References

Ashmore, J.F., and Copenhagen, D.R. (1983). An analysis of transmission from cones to hyperpolarizing bipolar cells in the retina of the turtle. J. Physiol. *340*, 569–597.

Attwell, D., Werblin, F.S., and Wilson, M. (1982). The properties of single cones isolated from the tiger salamander retina. J. Physiol. *328*, 259–283.

Attwell, D., Borges, S., Wu, S.M., and Wilson, M. (1987). Signal clipping by the rod output synapse. Nature *328*, 522–524.

Banks, M.S., Geisler, W.S., and Bennett, P.J. (1987). The physical limits of grating visibility. Vision Res. *27*, 1915–1924.

Barnes, S., and Hille, B. (1989). Ionic channels of the inner segment of tiger salamander cone photoreceptors. J. Gen. Physiol. *94*, 719–743.

Barnes, S., Merchant, V., and Mahmud, F. (1993). Modulation of transmission gain by protons at the photoreceptor output synapse. Proc. Natl. Acad. Sci. USA *90*, 10081–10085.

Berntson, A., and Taylor, W.R. (2003). The unitary event amplitude of mouse retinal on-cone bipolar cells. Vis. Neurosci. *20*, 621–626.

Bowen, R.W., Pokorny, J., and Smith, V.C. (1998). Sawtooth contrast sensitivity: decrements have the edge. Vision Res. *29*, 1501–1509.

Calkins, D.J., Schein, S.J., Tsukamoto, Y., and Sterling, P. (1994). M and L cones in macaque fovea connect to midget ganglion cells by different numbers of excitatory synapses. Nature *371*, 70–72.

DeMarco, P.J., Jr., Smith, V.C., and Pokorny, J. (1994). Effect of sawtooth polarity on chromatic and luminance detection. Vis. Neurosci. *11*, 491–499.

Demb, J.B., Sterling, P., and Freed, M.A. (2004). How retinal ganglion cells prevent synaptic noise from reaching the spike output. J. Neurophysiol. *92*, 2510–2519.

Derrington, A.M., and Lennie, P. (1984). Spatial and temporal contrast sensitivities of neurones in lateral geniculate nucleus of macaque. J. Physiol. *357*, 219–240.

DeVries, S.H. (2001). Exocytosed protons feedback to suppress the Ca^{2+} current in mammalian cone photoreceptors. Neuron *32*, 1107–1117.

Euler, T., Detwiler, P.B., and Denk, W. (2002). Directionally selective calcium signals in dendrites of starburst amacrine cells. Nature *418*, 845–852.

Gaal, L., Roska, B., Picaud, S.A., Wu, S.M., Marc, R., and Werblin, F.S. (1998). Postsynaptic response kinetics are controlled by a glutamate transporter at cone photoreceptors. J. Neurophysiol. *79*, 190–196.

Geisler, W.S. (1989). Sequential ideal-observer analysis of visual discriminations. Psychol. Rev. *96*, 267–314.

Harata, N., Ryan, T.A., Smith, S.J., Buchanan, J., and Tsien, R.W. (2001). Visualizing recycling synaptic vesicles in hippocampal neurons by FM 1-43 photoconversion. Proc. Natl. Acad. Sci. USA *98*, 12748–12753.

Hayhoe, M.M., Levin, M.E., and Koshel, R.J. (1992). Subtractive processes in light adaptation. Vision Res. *32*, 323–333.

Henkel, A.W., Lubke, J., and Betz, W.J. (1996). FM1-43 dye ultrastructural localization in and release from frog motor nerve terminals. Proc. Natl. Acad. Sci. USA *93*, 1918–1923.

Klingauf, J., Kavalali, E.T., and Tsien, R.W. (1998). Kinetics and regulation of fast endocytosis at hippocampal synapses. Nature *394*, 581–585.

Kreft, M., Krizaj, D., Grilc, S., and Zorec, R. (2003). Properties of exocytotic response in vertebrate photoreceptors. J. Neurophysiol. *90*, 218–225.

Krizaj, D., Lai, F.A., and Copenhagen, D.R. (2003). Ryanodine stores and calcium regulation in the inner segments of salamander rods and cones. J. Physiol. *547*, 761–774.

Maple, B.R., Werblin, F.S., and Wu, S.M. (1994). Miniature excitatory postsynaptic currents in bipolar cells of the tiger salamander retina. Vision Res. *34*, 2357–2362.

Normann, R.A., and Werblin, F.S. (1974). Control of retinal sensitivity. I. Light and dark adaptation of vertebrate rods and cones. J. Gen. Physiol. *63*, 37–61.

Parsons, T.D., and Sterling, P. (2003). Synaptic ribbon. Conveyor belt or safety belt? Neuron *37*, 379–382.

Patel, A.S., and Jones, R.W. (1968). Increment and decrement visual thresholds. J. Opt. Soc. Am. *58*, 696–699.

Perlman, I., and Normann, R.A. (1998). Light adaptation and sensitivity controlling mechanisms in vertebrate photoreceptors. Prog. Retin. Eye Res. *17*, 523–563.

Purves, D., Williams, S.M., Nundy, S., and Lotto, R.B. (2004). Perceiving the intensity of light. Psychol. Rev. *111*, 142–158.

Pyle, J.L., Kavalali, E.T., Piedras-Renteria, E.S., and Tsien, R.W. (2000). Rapid reuse of readily releasable pool vesicles at hippocampal synapses. Neuron *28*, 221–231.

Rabl, K., Cadetti, L., and Thoreson, W.B. (2005). Kinetics of exocytosis is faster in cones than in rods. J. Neurosci. *25*, 4633–4640.

Rea, R., Li, J., Dharia, A., Levitan, E.S., Sterling, P., and Kramer, R.H. (2004). Streamlined synaptic vesicle cycle in cone photoreceptor terminals. Neuron *41*, 755–766.

Renger, J.J., Egles, C., and Liu, G. (2001). A developmental switch in neurotransmitter flux enhances synaptic efficacy by affecting AMPA receptor activation. Neuron *29*, 469–484.

Richards, D.A., Guatimosim, C., Rizzoli, S.O., and Betz, W.J. (2003). Synaptic vesicle pools at the frog neuromuscular junction. Neuron *39*, 529–541.

Rieke, F., and Schwartz, E.A. (1994). A cGMP-gated current can control exocytosis at cone synapses. Neuron *13*, 863–873.

Rodieck, R.W. (1998). The First Steps in Seeing (Sunderland, MA: Sinauer Associates, Inc.).

Savchenko, A., Barnes, S., and Kramer, R.H. (1997). Cyclic-nucleotide-gated channels mediate synaptic feedback by nitric oxide. Nature *390*, 694–698.

Schnapf, J.L., Nunn, B.J., Meister, M., and Baylor, D.A. (1990). Visual transduction in cones of the monkey *Macaca fascicularis*. J. Physiol. *427*, 681–713.

Singer, J.H., Lassova, L., Vardi, N., and Diamond, J.S. (2004). Coordinated multivesicular release at a mammalian ribbon synapse. Nat. Neurosci. *7*, 826–833.

Stevens, C.F., and Williams, J.H. (2000). "Kiss and run" exocytosis at hippocampal synapses. Proc. Natl. Acad. Sci. USA *97*, 12828–12833.

Thoreson, W.B., Rabl, K., Townes-Anderson, E., and Heidelberger, R. (2004). A highly Ca^{2+}-sensitive pool of vesicles contributes to linearity at the rod photoreceptor ribbon synapse. Neuron *42*, 595–605.

Verweij, J., Kamermans, M., and Spekreijse, H. (1996). Horizontal cells feed back to cones by shifting the cone calcium-current activation range. Vision Res. *36*, 3943–3953.

Vessey, J.P., Stratis, A.K., Daniels, B.A., Da Silva, N., Jonz, M.G., Lalonde, M.R., Baldridge, W.H., and Barnes, S. (2005). Proton-mediated feedback inhibition of presynaptic calcium channels at the cone photoreceptor synapse. J. Neurosci. *25*, 4108–4117.

Wu, S.M. (1994). Synaptic transmission in the outer retina. Annu. Rev. Physiol. *56*, 141–168.

Zenisek, D., Steyer, J.A., and Almers, W. (2000). Transport, capture and exocytosis of single synaptic vesicles at active zones. Nature *406*, 849–854.

Zenisek, D., Horst, N.K., Merrifield, C., Sterling, P., and Matthews, G. (2004). Visualizing synaptic ribbons in the living cell. J. Neurosci. *24*, 9752–9759.